

## More about the Ordovician–Silurian transition beds at Mirny Creek, Omulev Mountains, NE Russia: carbon isotopes and conodonts

Dimitri Kaljo, Peep Männik, Tõnu Martma and Jaak Nõlvak

Institute of Geology at Tallinn University of Technology, Ehitajate tee 5, 19086 Tallinn, Estonia; kaljo@gi.ee

Received 4 July 2012, accepted 15 October 2012

**Abstract.** Profound environmental and biodiversity changes take place in the Ordovician–Silurian boundary interval. The Mirny Creek and Neznakomka River bank sections discussed in this paper expose the upper Katian–lower Rhuddanian part of the boundary beds. The succession consists of carbonate rocks, partly with bioherms, alternating with argillaceous and siltstone packages that are well dated by graptolites. Microfossils are rare, especially in the Hirnantian, but conodonts provide some useful markers just below and above the Hirnantian stage boundaries. The Hirnantian  $\delta^{13}\text{C}$  trend in the Mirny Creek section is the stratigraphically longest described so far and it has a highly specific shape. The trend commenced at the first appearance datum of *Normalograptus extraordinarius* or slightly below this level. The main peak occurs near the middle of the *N. persculptus* Biozone. Samples from the Neznakomka River suggest a somewhat wider peak interval than at Mirny Creek. Detailed comparison of the Mirny and Stirnas (Latvia)  $\delta^{13}\text{C}$  curves shows a general similarity despite great specific features of both trends. Correlation of the  $\delta^{13}\text{C}$  trends from China, Baltica and North America with that at Mirny Creek reveals a great variety of shapes of the carbon isotope curve. However, its rising limb commenced, if represented, everywhere close to the beginning of the *N. extraordinarius* Biozone or in terms of the Baltic succession, at the bottom of the Porkuni Regional Stage. Most likely a general shape of the HICE trend is pyramidal, which is peaking in the early *N. persculptus* Biochrone. Differences in the values and shape of an actual curve at different localities depend on local environmental conditions, sometimes modifying the global signal rather strongly.

**Key words:** Hirnantian, carbon isotopes, graptolites, conodonts, Mirny Creek, NE Russia.

### INTRODUCTION

System boundaries are commonly objects of high interest, and the Ordovician–Silurian (below O/S) boundary is not an exception. This interval includes some profound environmental and biodiversity changes in general and diversified details at a closer look. The cornerstone of the puzzle related to the O/S transition is the Hirnantian Stage, which is characterized by complicated processes, such as one or more glacial events, mass extinctions in biota, and carbon and oxygen isotope variations. Most of these events, however, had their roots in pre-Hirnantian time and continued into the Silurian. Therefore, although focusing mainly on the Hirnantian part of the section, we also include in our analysis data from the over- and underlying strata.

Some three decades ago the Hirnantian part of the section at Mirny Creek played an important role in the discussions concerning the lower boundary of the Silurian System. The study history and the modern state of knowledge about the section were reviewed by Koren' & Sobolevskaya (2008). Based mainly on that paper and our new carbon isotope and conodont data, we will

discuss some aspects of regional stratigraphy and a couple of more general topics of the uppermost Ordovician isotope geology, first of all differences in patterns of the  $\delta^{13}\text{C}$  trends in Avalonia, Baltica, Laurentia, the South China plate and Kolyma terrain, correlation of bio- and chemostratigraphic events, and dating of carbon isotope excursions in terms of biostratigraphy. The story of the last terrain is less studied than others, but some data refer to its location close to Laurentia during late Ordovician time and much later accretion to the east of Siberia (Rong & Harper 1988; Cocks & Torsvik 2004).

The studied Mirny Creek and Neznakomka River sections include exposures of the upper Katian through lower Rhuddanian. Conodont associations identified in this interval are poor to very poor, and conodonts are almost missing in the Hirnantian (Zhang & Barnes 2007, see also our data below). Chitinozoans, except rare poorly preserved fragments, were not found. Shelly fossils like brachiopods and trilobites are quite common at some levels, but graptolites play a leading role in biostratigraphy and are used for the establishment of a clear general biozonal framework of the Mirny section (Koren' & Sobolevskaya 2008). Despite the occurrence

of mixed shelly–graptolite assemblages in the studied section, detailed correlation with shelly faunal successions in the Baltic and some other regions is problematic due to scarcity of microfossils. Referring to continued debates about the ‘age of the *taugourdeui* Biozone’ (Melchin & Holmden 2006; Kaljo et al. 2008; Achab et al. 2011), we note that chemostratigraphic correlation criteria are surely most helpful in achieving reliable results. Recent advancements in many areas, including Anticosti Island (Achab et al. 2011; Jones et al. 2011), Baltica (Schmitz & Bergström 2007; Kaljo et al. 2008; Ainsaar et al. 2010; Hints et al. 2010; Bergström et al. 2012) and China (Chen et al. 2006; Zhang et al. 2009; Gorjan et al. 2012), provide a good basis for such a discussion. Based on these and data from Dob’s Linn (Underwood et al. 1997) and Nevada (Finney et al. 1999; Kump et al. 1999; LaPorte et al. 2009), we wish to refine the understanding of the Hirnantian  $\delta^{13}\text{C}$  trend and its global utility as a chronostratigraphic tool integrated with different kinds of biostratigraphy. On the other hand, the Hirnantian succession in the Mirny Creek area is 4–5 times thicker than in the East Baltic and more than 100 times thicker than in some Chinese (for example Wangjiawan North) sections. Considering the very rapid sedimentation in the Mirny Creek area, we do think that certain differences in the general shape of the  $\delta^{13}\text{C}$  excursion (Kaljo & Martma 2011) should be checked for a rational explanation that might be linked to environmental parameters of the region.

## GEOLOGICAL SETTING

Mirny Creek is a small tributary of the Omulevka River belonging to the Kolyma River basin at  $64^\circ\text{N}$  ca 700 km north of Magadan (Fig. 1). The outcrops on both banks of the creek serve as a key section for the Omulev Mountain region, showing an almost continuous succession of the Middle Ordovician to lower Devonian strata, thoroughly described by Oradovskaya & Sobolevskaya (1979) and Koren’ et al. (1983).

The Mirny Creek and Neznakomka River sections, discussed in this paper, embrace the upper Katian through the Rhuddanian (Fig. 2), representing a rather thick succession (ca 400 m) of rapidly accumulated carbonate sediments alternating with argillaceous and siltstone packages (Koren’ et al. 1983). The section displays a diversity of facies, from deep-water graptolite shale to outer shelf brachiopod-coral-graptolite-bearing carbonates, locally with bioherms. The sedimentary strata are partly strongly folded and faulted, some intervals are covered and some contacts are tectonic (Oradovskaya & Sobolevskaya 1979). Still, the primary authors cited above and Koren’ & Sobolevskaya (2008) showed that the succession of the study interval is not seriously disturbed at key levels and is biostratigraphically continuous. The conodont colour alteration index (CAI 4–5) indicates (Nowlan & Barnes 1987) that the rocks are thermally altered. Microfossils are quite rare, but graptolites are of greatest significance, providing a highly distinct

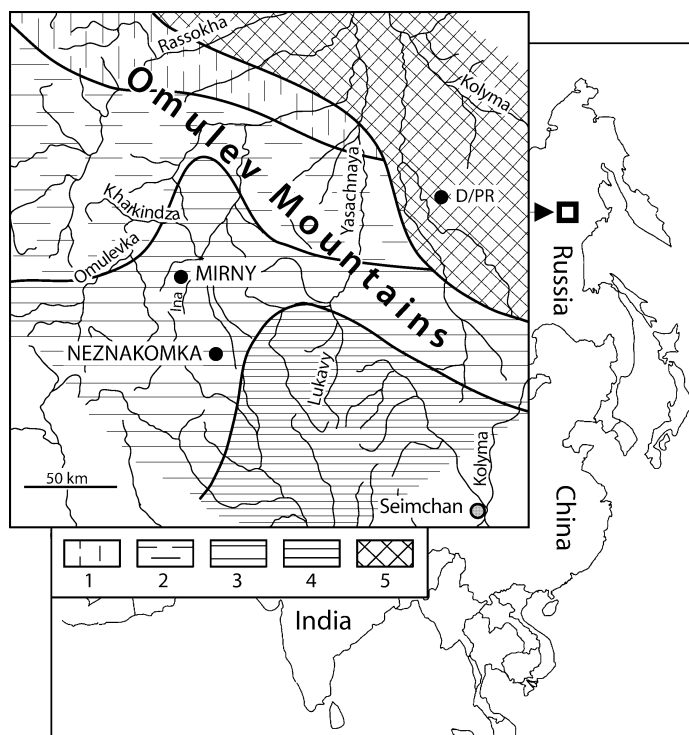


**Fig. 1.** Location of the two studied sections (black dots) in the Omulev Mountains area, NE Russia, on the background of late Ordovician facies zones according to Koren’ et al. (1983). Key: 1, nearshore trachytes, breccias and limestones; 2, dolomitic limestones and marls formed in lagoons behind reefs; 3, upper slope belt of skeletal, silty and conglomeratic limestones with small bioherms (individually not shown); 4, lower slope belt with calcareous–argillaceous shales and limestones; 5, land. D/Pr, Devonian rocks overlie Precambrian.

System	Series	Stage	Graptolite biozone	Regional stage	Formation	Unit	Member	Conodont biozone	
Silurian	Llandovery	Rhuddanian	<i>cyphus</i>	Chalmak	Maut	S	81	<i>kentuckyensis</i>	
			<i>vesiculosus</i>			R	78		
			<i>acuminatus-ascensus</i>				77		
							74 73		
Ordovician	Upper	Hirnantian	<i>persculptus</i>	Tirekhtyakh	Tirekhtyakh	Q	72	<i>ordovicianus</i>	
						69			
		<i>extra-ordinarius</i>				68			
			67						
	Katian	<i>supernus</i>					P	66 65	?
							O	64	
								60	
							N	59	
								55	
							M	54	
		<i>quadrimucronatus</i>	Padun	Padun			53	?	
						51			

**Fig. 2.** Stratigraphy of the upper Ordovician and lowermost Silurian of the study area in NE Russia. The scheme is based on Koren' et al. (1983) with modifications according to Koren' & Sobolevskaya (2008) and Zhang & Barnes (2007).

general biozonal framework for the Mirny Creek section and correspondingly enabling also the time correlation with global standard stratigraphy (Koren' & Sobolevskaya 2008).

Figure 2 presents the local and other stratigraphical terminology used in the paper. Besides common terms like biozone, formation, stage and series, it contains two terms (unit, member) introduced by Oradovskaya & Sobolevskaya (1979) and followed by others. According to a Russian stratigraphical code (Zhamoida 1992), these terms, in Russian called, respectively, 'tolshcha' and 'pachka', are lithostratigraphic units of approximately formation (tolshcha) and its subdivision rank, but insufficiently studied. Thus we prefer to employ 'unit', following the pioneer authors at Mirny Creek. We will also use 'member', which seems to mean more 'a description unit for a group of similar beds'.

## MATERIAL AND METHODS

Most of the samples used for this study were collected in 1978 by our former colleague, sedimentologist Lembit

Põlma (1934–1988) during a wider study of the O/S boundary beds in this area (Koren' et al. 1983). He studied the lithology of the sections and took samples in order to characterize different types of rocks, thus at irregular intervals. Although most of his samples were rather big, the main part of each was used to prepare a polished slab. On the basis of L. Põlma's field notes we could locate the samples in the section. Additionally, several samples, collected by T. N. Koren' during field work in the area and by D. Kaljo during the O/S working group excursion in 1979, were studied. To confirm some local correlations, we examined also nine samples from the Neznakomka River section. Carbon isotopes were analysed in 57 samples from the uppermost Katian to the lowermost Rhuddanian interval by using standard methods outlined below. Most of L. Põlma's samples were earlier analysed also chemically in order to elucidate the content of calcite, dolomite and terrigenous material. All analytical data are presented in Table 1, and  $\delta^{13}\text{C}$  values together with the most substantial macrofossil occurrences in Fig. 3.

The sampling levels (calculated depths) referred to in Table 1 and below in the text were found on the basis of the measured thicknesses of strata. Mean intervals between samples in the Hirnantian part of the section are 3.2 m (corresponds to ca 70 Ka according to the absolute timescale by Webby et al. 2004). Fortunately, the most interesting intervals (the Katian–Hirnantian boundary and the interval of mid-*persculptus*  $\delta^{13}\text{C}$  peak values) were sampled in slightly more detail: one sample every 2 m.

Acid-resistant microfossils were studied only in the late Katian to Rhuddanian samples from the Mirny Creek section. In terms of regional stratigraphy, this interval corresponds to the uppermost Padun, Tirekhtyakh and lower Maut formations (Fig. 2). For microfossil study leftovers of 47 lithological samples collected by L. Põlma in 1978 were processed. The actual amount of rock available for processing varied largely, from 34 g (sample 110-2/1) to 823 g (sample 107-6/1), but most of the samples were between 100 and 300 g. In addition, four samples collected by D. Kaljo in 1979 were processed. The content of terrigenous material in the samples is highly variable (e.g. Koren' et al. 1983: fig. 13; see also Table 1 for samples by Põlma). Samples with a low content of terrigenous material dissolved relatively easily, while those with a high content of terrigenous material dissolved very poorly or not at all. The samples were processed using standard methods: first with buffered acetic acid, then with buffered formic acid. The samples which did not react with any of these acids were disintegrated mechanically using sodium hyposulphite. In some cases even this method did not

**Table 1.** Carbon isotope and geochemical data from the Mirny Creek and Neznakomka River sections. Calculated depth explained in the ‘Material and methods’ section

No.	Unit	Member	Sample No. (original)	Calculated depth, m	$\delta^{13}\text{C}$ , ‰	Calcite, %	Dolomite, %	Terrigenous material, %
Mirny Creek								
1	R	74	109-2/5	2	-2.1			
2	R	74	109-2/3	4	-0.88			
3	R	74	109-2/2	6	1.16	78.5	8.5	13.0
4	R	74	109-2/1	8	1.51	58.4	4.8	36.8
5	R	73	109-1/2	10	0.29			
6	R	73	109-1/1	10.5	-0.07			
7	Q	72	107-6/3	11.5	-0.28	7.7	39.5	52.7
8	Q	72	107-6/2b	12	0.66			
9	Q	72	107-6/2a	12.5	0.37	11.1	36.0	58.9
10	Q	72	107-6/1tum	13	1.06	7.5	31.9	60.6
11	Q	72	107-6/1hel	13.5	0.27	10.1	19.4	70.5
12	Q	71	107-5/7	17	0.44			
13	Q	71	107-5/4	20	1.07	11.7	30.0	58.3
14	Q	71	107-5/3	24	0.95	20.2	18.2	61.6
15	Q	71	107-5/6	27	1.14			
16	Q	71	107-5/2	30	1.31	27.0	18.4	54.6
17	Q	71	107-5/1	32	1.20	17.1	23.3	59.6
18	Q	70	107-4/5	35	5.36	81.3	7.7	11.0
19	Q	70	107-4/4	37	4.37	60.5	12.1	27.4
20	Q	70	107-4/3	38	3.73	57.3	12.9	29.8
21	Q	70	107-4/2	39	1.19	15.8	24.3	59.9
22	Q	70	107-4/1	41	1.60	39.8	19.1	41.1
23	Q	69	107-3/5	46	1.19			
24	Q	69	107-3/2	49	0.79	13.2	18.9	67.9
25	Q	69	107-3/4	53	1.93			
26	Q	68	107-2/4	66	1.41	16.0	30.6	53.4
27	Q	68	107-2/5	69	1.48			
28	Q	68	D-4	82	1.42			
29	Q	68	D-3	88	1.66			
30	Q	68	107-2/1	91	1.46	11.3	29.2	59.5
31	Q	67	107-1/3	96	1.64	91.9	1.7	6.4
32	Q	67	107-1/2	97	2.75	85.4	2.8	11.8
33	Q	67	107-1/1b	98	2.96	67.4	4.1	28.5
34	Q	67	107-1/1a	99	1.58	59.7	1.2	39.1
35	P	66	108-2/5	101	0.83	14.5	7.3	78.2
36	P	66	108-2/3b	103	0.34			
37	P	66	108-2/3a	104	1.02	10.5	14.5	75.0
38	P	66	108-2/2	105	1.04			
39	P	65	108-1/2b	111	-1.22			
40	O	64	D-1	122	1.60	73.9	3.3	22.8
41	O	63	112-5/4	132	0.55	70.4	4.7	24.9
42	O	63	112-5/2	135	0.77			
43	O	62	112-4/1	147	1.27	81.9	3.4	14.7
44	O	61	112-3/1	152	1.04	33.5	2.3	64.2
45	O	61	112-3/1T	152	0.86			
46	O	61	112-3/1T	152	0.91	75.7	4.0	20.3
47	O	59	112-1/2	161	1.31			
48	O	59	112-1/1	162	1.21	89.4	3.8	6.8
Neznakomka River								
49	Maut Fm.	10	9-5a		0.34	90.8	5.0	4.2
50	Maut Fm.	9	9-4b		1.18	85.3	14.0	0.8
51	Maut Fm.	8	9-3b		0.32	89.1	3	7.9
52	Upper Tirekhtyakh Fm.	5	7-4b		4.8	72.1	8.9	19.0
53	Upper Tirekhtyakh Fm.	5	7-4a		4.9	88.8	5	6.2
54	Upper Tirekhtyakh Fm.	4	7-3b		2.5	16.1	43.9	40
55	Upper Tirekhtyakh Fm.	4	7-3a		1.9	14.1	29.1	56.8
56	Upper Tirekhtyakh Fm.	3	7-1b		0.33	2.8	24.1	73.1
57	Upper Tirekhtyakh Fm.	3	7-1a		0.06	4.1	32.1	63.8

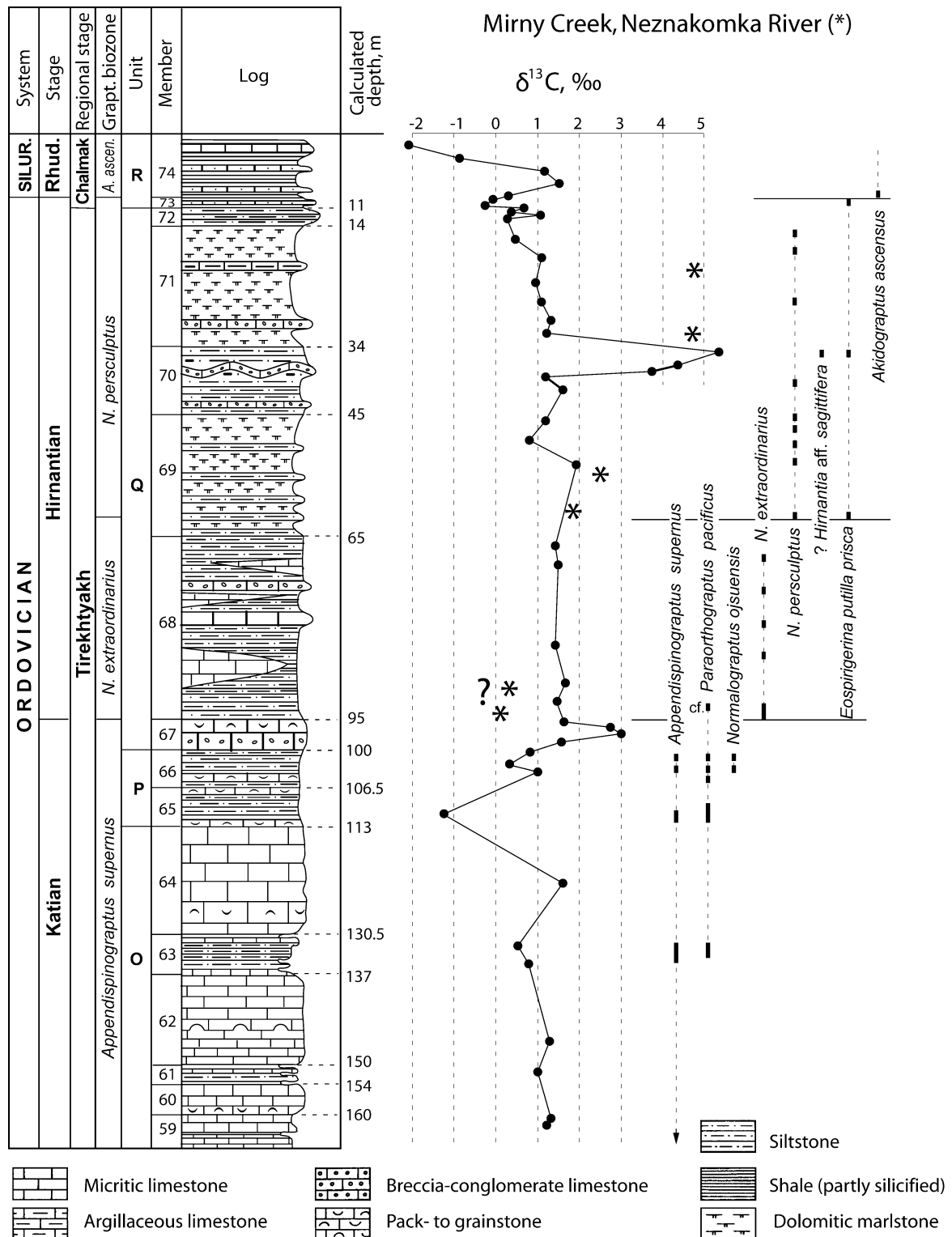


**Fig. 3.** Lithological log, stratigraphical subdivisions, fossil occurrences (all based on Koren' et al. 1983; Koren' & Sobolevskaya 2008) and carbon isotope trend measured in the Ordovician–Silurian rocks of the Mirny Creek section with additions from the Neznakomka River outcrops. Note the question mark at the two lowest Neznakomka samples casting doubt about the position.

help much. All residues were checked for chitinozoans and other bioclasts while still wet, then they were dried and picked for conodonts. Most of the residues were too large to be picked directly and were separated by heavy liquid before picking. Only a few very poorly preserved (unidentifiable) chitinozoan and scolecodont remains were found. Very rare occurrence of these usually quite common fossils indicates that most of them were evidently destroyed during tectonic and thermal alteration of rocks. Also, considering the great thickness of strata (high sedimentation rate), obviously the samples were too small. This may have been the case with conodonts, which were found in 31 of 51 processed samples. The majority of the productive samples yielded just a few specimens, only rarely more. In total, 333 identifiable conodont specimens of variable preservation (mostly broken) were found.

Carbon isotope analyses were performed in the Laboratory of Mass Spectrometry, Institute of Geology at Tallinn University of Technology, using a standard method explained in more detail in Kaljo et al. (1997) and Martma et al. (2005). Here we note only that whole-rock samples were crushed, the material was powdered and treated with 100% phosphoric acid at 100 °C for 15 min and analysed with the Delta V Advantage mass spectrometer with the GasBench II preparation line. All results were checked regularly against laboratory control samples and international standards. The results are given in the usual  $\delta$ -notation, as per mil deviation from the VPDB standard. Reproducibility of replicate analyses was generally better than 0.1‰.

All rock samples, residues and conodont elements studied for this paper are deposited at the Institute of Geology at Tallinn University of Technology (abbreviated as GIT). For the figured specimens the collection number 652 is allocated. Rock samples belong to a collection by L. Põlma (GIT 156). Information on individual samples (original numbers quoted in Table 1) can be obtained from the on-line catalogue at <http://sarv.gi.ee>.

## RESULTS

### Carbon isotope excursions, Mirny Creek

The Katian part of the  $\delta^{13}\text{C}$  excursion, except the uppermost portion (Unit P, Fig. 3), is substantiated by too widely spaced samples in order to be a trusted curve, but still the general trend is rather stable, varying close to 1‰ (0.6–1.3‰). Only two neighbouring samples (Nos 39 and 40, but 10 m away from each other) show diverging values that cannot be plausibly interpreted.

The two topmost samples (Nos 35 and 36) of Unit P and the first two samples (Nos 33 and 34) of Unit Q show a rather quick increase in  $\delta^{13}\text{C}$  values from 0.3‰

to 3.0‰ and then 2.8‰. They form the first clear medium-sized peak of values identified in the uppermost Ordovician of the Mirny Creek section. Higher in the section carbon isotope values slightly decrease and form a relatively even (1.4–1.7‰) long, slightly elevated plateau, which reaches, after a 13 m sampling gap, a little increased value (1.9‰) at 53 m depth. The next four samples (Nos 21–24) show rather variable  $\delta^{13}\text{C}$  values (0.8–1.6‰), which could be considered as the end of the above noted long plateau.

The highest  $\delta^{13}\text{C}$  values (3.7–5.4‰) in the Mirny Creek section were measured in the next three samples (Nos 18–20), surely marking the peak of the well-known Hirnantian carbon isotope excursion (HICE) at 34 m depth within Member 70. The peak is followed by a steep decrease in values (about 4‰) down to nearly 1.2‰. Then the excursion continues as a nearly horizontal or a very slowly falling plateau remaining close to 1‰ at 20 m depth.

The topmost 3 m of the Tirekhtyakh Formation (Member 72) show highly variable  $\delta^{13}\text{C}$  values (–0.28‰ to 1.1‰, mean value 0.4‰ from five measurements). The Silurian Maut Formation begins (Member 73) with even lower values (mean 0.1‰ from two samples) at the very bottom, but a low positive  $\delta^{13}\text{C}$  shift (1.5‰) occurs a little higher (Member 74), followed by a steep drop of values down to –2.1‰.

From the above data we observe the following patterns of the  $\delta^{13}\text{C}$  trend (Fig. 3): (1) a Katian plateau of low  $\delta^{13}\text{C}$  values varying close to 1‰ in Unit O; (2) a brief interval of increasing values in the top of Unit P ending with a medium-size peak (3‰) at the very beginning of Unit Q (Member 67); (3) a plateau of slightly elevated values varying close to 1.5‰ in the lower part of Unit Q; (4) a narrow peak of  $\delta^{13}\text{C}$  values (maximum value 5.4‰) in the middle of Unit Q; (5) a short falling plateau and a low of values at the O/S boundary, followed by a minor positive excursion (1.5‰) in the lowermost Silurian.

Key levels of the above Mirny Creek carbon isotope data curve are reliably dated by graptolites (Koren' & Sobolevskaya 2008). The upper Katian part of the curve belongs to the *Appendispinograptus supernus* Biozone (highest occurrences in members 65 and 66). Identification of the Katian–Hirnantian boundary level within the Tirekhtyakh Formation is more problematic (see 'Discussion' below). Without going into details, we quote *Normalograptus extraordinarius* as occurring at 95 m depth just above a pack- and grainstone bed at the very bottom of Unit Q (Fig. 3). This bed shows a typical 'rising limb' of the HICE. The upper boundary of the Hirnantian or the O/S boundary is well defined by the FAD of *Akidograptus ascensus* in the lowermost part of the Maut Formation (Member 74) but the HICE ends probably in Member 72.

### Neznakomka River banks

Having seen a rather specific carbon isotope trend in the Mirny Creek section (Figs 1, 3), we tried to find some additional data from the same area. Samples collected by L. Põlma from the Neznakomka River seemed most promising, but their number was insufficient for compiling a normal  $\delta^{13}\text{C}$  curve. According to Koren' et al. (1983), the thickness of the Hirnantian rocks at the Neznakomka River belonging to the upper part of the Tirekhtyakh Formation is 95 m. From these beds we analysed six samples taken mostly at an interval of 15–20 m; only the two lowermost ones are close to each other (2 m interval). These data are shown in Fig. 3 together with the curve from the Mirny Creek section. Due to possible correlation errors, we cannot be sure that the Neznakomka River analyses are shown in precisely correct positions. Nevertheless, these samples provided valuable information (Table 1) for interpreting the Mirny Creek section.

The first two samples at the bottom of Bed 3 near the first occurrences of *N. extraordinarius* gave very low  $\delta^{13}\text{C}$  values close to 0 but still show a certain increase upwards (actual position of samples is doubtful). Several samples higher in the section indicate a clear rising trend of  $\delta^{13}\text{C}$  values, e.g. the value 1.9‰ was measured 30 m above the FAD of *N. extraordinarius* in Bed 4 and 2.5‰, 10 m higher. The trend continued in Bed 5 (constitutes the uppermost 35 m of the Tirekhtyakh Formation) – a sample 20 m higher gave the value 4.9‰ and another sample, 18 m higher, the value 4.8‰. Three samples from the Maut Formation (Silurian) are irrelevant to our topic. All analyses of Unit Q represent a clear major  $\delta^{13}\text{C}$  excursion, but because of the scarcity of samples we cannot be sure about the real shape of the isotope curve. Anyway, it is obvious that the HICE peak at the Neznakomka River is much wider than that in the Mirny section. If two samples in Bed 5 constitute the main peak of the HICE, the peak occurs very high in the Neznakomka River section and may suggest a gap within the top of the Tirekhtyakh Formation or complications in the sedimentary process and correlation.

### Microfossil abundance and diversity

We processed 51 samples from the Mirny Creek section, covering the interval from the uppermost Padun Formation (Unit M, Member 51) up to Unit S (Member 81) of the Maut Formation. Nearly 40% of the samples did not contain any bioclasts. The share of barren samples was highest in the Hirnantian part of the section (Unit Q) where only two samples of nine were productive, both yielding a single conodont specimen. As a rule, also

non-barren samples in the section are very poor – only five samples produced more than ten conodont specimens (Fig. 4). Scarcity of conodonts in the Mirny Creek section was demonstrated also by Zhang & Barnes (2007). All other groups are represented as a rule by single elements or fragments per sample, e.g. chitinozoans only in six samples (*Cyathochitina* and *Conochitina* sp. indet. are possible) within members 59–68 belonging to the upper Katian and lowermost Hirnantian. Scolecodont fragments were found in nine samples, mostly in members 59–63 (Katian) and 77–79 (mid-Rhuddanian), but one fragment also in Member 70 (HICE peak interval). Rare occurrence of chitinozoans and scolecodonts may be (partly) explained by strong heating of rocks in the section (as evidenced by CAI 4–5 = 300–400 °C). The Silurian part of the section seems to contain a more abundant and diverse fossil assemblage, including in addition to the microfossils listed above also 1–4 fragments of graptolites, ostracodes, inarticulate brachiopods and some sponge spicules.

Comparison of the abundance and diversity by groups of microfossils revealed that only conodonts are represented by at least one element in 65% of the samples and thus deserved closer biostratigraphical attention (see below). This abundance rate is rather poor, but still some distribution patterns could be noted. Conodonts are more common in the Katian and Rhuddanian but extremely rare in the Hirnantian strata (Fig. 4). The same pattern is also followed by other groups of microfossils, but not by macrofossils. The Hirnantian is the most dolomite-rich part of the studied section (Koren' et al. 1983). That may have affected calcitic skeletons and chitinozoans (pers. comm. by Jaak Nõlvak and Viuu Nestor), but this is an improbable reason for selective destruction of all organic microremains.

### Conodont assemblage: taxonomic composition, affinities and biostratigraphy

As noted above, among microfossils only conodonts, although rare, are preserved well enough to be identifiable. When studying the Mirny Creek section, Zhang & Barnes (2007) processed 23 samples from the stratigraphic interval discussed in this paper. Nineteen of their samples appeared to be productive and yielded a total of 570 identifiable conodont specimens. The average weight of the samples processed by Zhang & Barnes (2007) was ca 2 kg. Their data (approximate positions of samples and distribution of identified taxa) are included in Fig. 4.

The Mirny Creek section was sampled by C. Barnes, but rather irregularly (Fig. 4). He was probably looking for lithologies promising for conodont studies, while L. Põlma tried to sample all lithologies. In both sets of

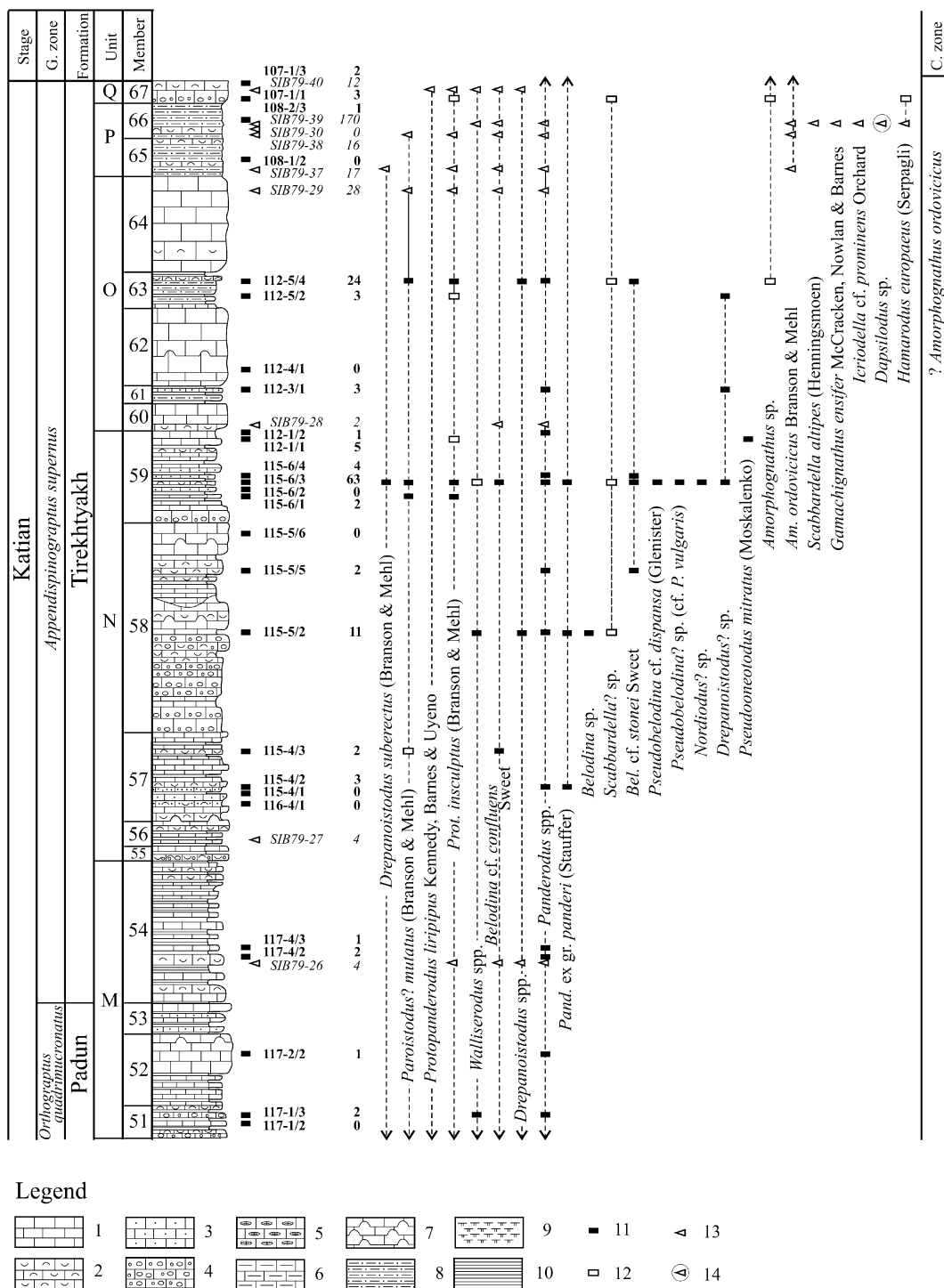


**Fig. 4.** Distribution of conodonts in the Mirny Creek section, including our data (black rectangles) and those by Zhang & Barnes (2007) (empty triangles). From left to right: global and regional stratigraphy; lithological log (modified from Koren' et al. 1983; stage boundaries after Koren' & Sobolevskaya 2008); position of samples; sample numbers; number of specimens per sample; distribution of taxa; conodont zonation. Legend: 1, limestone; 2, bioclastic limestone; 3, silty limestone; 4, conglomeratic limestone; 5, silicified limestone; 6, argillaceous limestone; 7, bioherms; 8, siltstone; 9, dolomitic marlstone; 10, argillaceous and/or silicified shale; 11, reliable identification of a taxon; 12, problematic identification of a taxon; 13, identification by Zhang & Barnes (2007); 14, revised identification of a taxon illustrated in Zhang & Barnes (2007). Abbreviations: G. zone, Graptolite zone; C. zone, Conodont zone; *Prot.*, *Protopanderodus*; *Pand.*, *Panderodus*; *Bel.*, *Belodina*; *Am.*, *Amorphognathus*; *Par.*, *Paroistodus*; *Oul.*, *Oulodus*; *Oz.*, *Ozarkodina*.

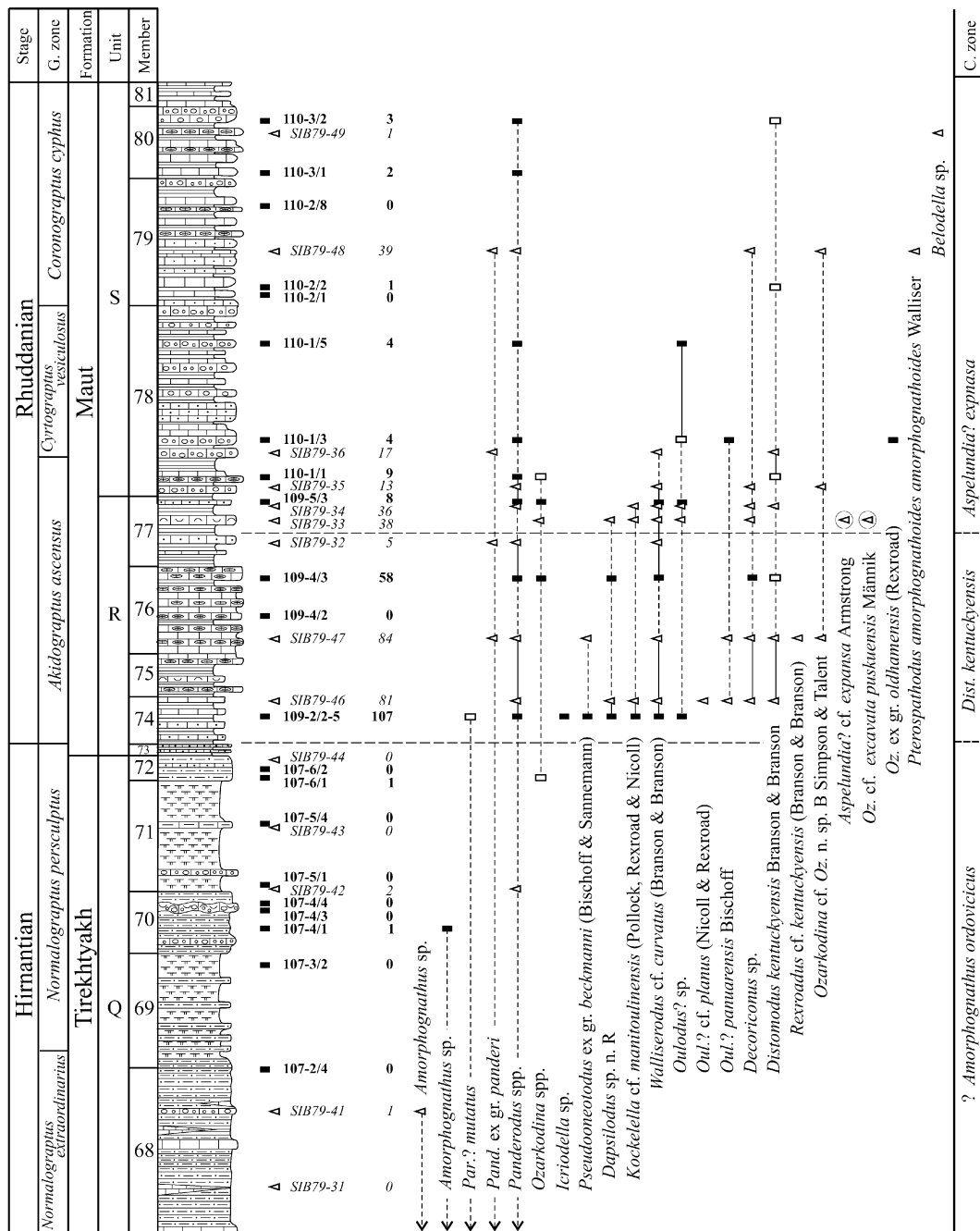


Fig. 4. Continued.

samples those from the uppermost Padun (members 51–53), lower to middle Tirekhtyakh (members 54–67) and lower Maut (members 74–80) formations, in other words, pre- and post-Hirnantian rocks, were productive. The upper Tirekhtyakh Formation, representing the Hirnantian (members 68–72), yielded only few fragments of *Amorphognathus* and a probable specimen of *Ozarkodina* sp.

The lower part of the studied section (uppermost Padun–middle Tirekhtyakh formations) contains a typical Upper Ordovician fauna. Taxa with simple-cone apparatuses (*Belodina*, *Drepanoistodus*, *Panderodus*, *Protopanderodus*, etc.) are the most common. *Amorphognathus* is very rare, being represented only in the upper part of the Tirekhtyakh Formation and, as a rule, mainly by fragments that Zhang & Barnes (2007) identified as *Eocarniodus gracilis*

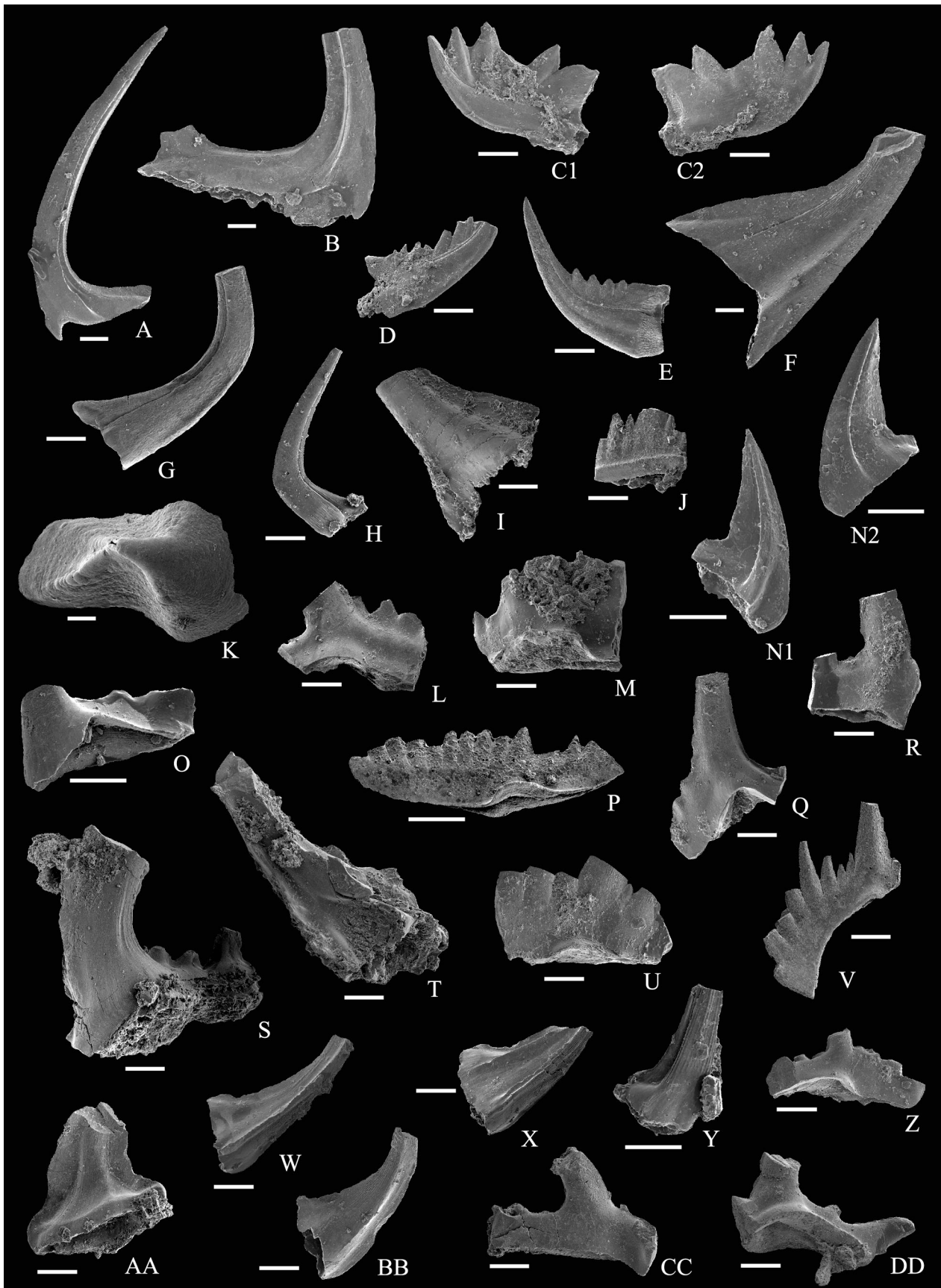
Rhodes. In reality, the specimens assigned to this taxon are fragments of *Amorphognathus*? S elements (their processes). Zhang & Barnes (2007) identified *A. ordovicicus* Branson & Mehl in their collection, although, as they indicate, no diagnostic M element was found. Unfortunately, our material is too poorly preserved to allow identification of this species (Fig. 5J). Anyhow, if the identification of *A. ordovicicus* by Zhang & Barnes (2007) is correct, at least the upper part of the Tirekhtyakh Formation (starting from Unit P) corresponds to the *A. ordovicicus* conodont Zone (Fig. 4). Zhang & Barnes (2007, fig. 7: 8) recognized in their sample SIB79-40 a probable specimen of *Aphelognathus*. However, based on their illustration, this seems to be a misinterpretation and, most probably, this fragment also belongs to *Amorphognathus*.

In their richest sample (SIB79-39, 170 specimens) from the middle part of the Tirekhtyakh Formation (Member 66) Zhang & Barnes (2007) identified *Gamachignathus ensifer* McCracken, Nowlan & Barnes, *Icriodella* cf. *I. prominens* Orchard and *Hamarodus europaeus* (Serpagli). The last taxon was also found in our sample 107-1/1, from the base of the overlying Member 67 (Fig. 5I). The specimens of *Scabbardella altipes* (Henningsmoen), illustrated from sample SIB79-39 by Zhang & Barnes (2007, fig. 8: 16–19), are problematic and seem to be more similar to elements of *Dapsilodus*. If this is the case, then sample SIB79-39 is the only one from the Ordovician part of the Mirny Creek section with *Dapsilodus*. *Scabbardella* (probably *S. altipes*)

occurs in several samples in the middle Tirekhtyakh Formation (Figs 4, 5F). Identification of *Panderodus* [excluding *P. panderi* (Stauffer)] on the basis of heated (dark) specimens with invisible internal structures (distribution of the basal cavity and white matter) is not reliable. Hence, identification of *P. unicostatus* (Branson & Mehl) by Zhang & Barnes (2007) is highly problematic, as is also the occurrence of *Walliserodus curvatus* (Branson & Branson) in the Tirekhtyakh Formation (and below in the Ordovician).

A rich conodont fauna appears in the lowermost Silurian in the basal Maut Formation (in Member 74) and is well represented also in the overlying strata up to Member 78. Higher in the section conodonts become rare. The Silurian assemblage consists of taxa characteristic of the Rhuddanian and (lower) Aeronian: *Distomodus* cf. *kentuckyensis* Branson & Branson (Fig. 5S, T), *Kockelella* cf. *manitoulinensis* (Pollock, Rexroad & Nicoll) (Fig. 5L, M, Q, R), *Ozarkodina* ex gr. *oldhamensis* Rexroad (Fig. 5P), *Oulodus?* *panuarensis* Bischoff (Fig. 5O), etc. Also several simple-cone taxa are found in this interval. However, the elements of *Dapsilodus obliquicostatus* (Branson & Mehl) illustrated by Zhang & Barnes (2007, fig. 9: 1–3) belong, in reality, to an older undescribed form of *Dapsilodus* occurring in the Rhuddanian–early Aeronian strata in the eastern Baltic (identified as *Dapsilodus* sp. n. R in Männik 2003 and Loydell et al. 2010). Similarly, *Decoriconus fragilis* (Branson & Mehl) in Zhang & Barnes (2007, fig 9: 10–15) is, most probably, an older representative of *Decoriconus*.

**Fig. 5.** Selected conodonts from the Mirny Creek section. Scale bar corresponds to 0.1 mm. **A, B**, *Protopanderodus insculptus*: A, lateral view of symmetric adenticulate acontiodontiform element, GIT 652-1; B, lateral view of asymmetric denticulate acontiodontiform element, GIT 652-2; both specimens from sample 115-6/3, Tirekhtyakh Formation. **C**, *Pseudobelodina?* sp. (cf. *P. vulgaris*), inner (C1) and outer (C2) lateral views of grandiform element, GIT 652-3, sample 115-6/3, Tirekhtyakh Formation. **D**, *Pseudobelodina* cf. *dispansa*, lateral view of compressiform element, GIT 652-4, sample 115-6/3, Tirekhtyakh Formation. **E**, *Belodina* cf. *stonei*, lateral view of compressiform element, GIT 652-5, sample 115-6/3, Tirekhtyakh Formation. **F**, *Scabbardella?* sp., lateral view of acodiform element, GIT 652-6, sample 115-6/3, Tirekhtyakh Formation. **G**, *Panderodus* ex gr. *panderi*, lateral view of high-based asymmetric graciliform element, GIT 652-7, sample 115-4/2, Tirekhtyakh Formation. **H**, *Panderodus* ex gr. *panderi*, lateral view of low-based symmetric graciliform element, GIT 652-8, sample 115-5/2, Tirekhtyakh Formation. **I**, *Hamarodus* cf. *europaes*, outer lateral view of P? element, GIT 652-9, sample 107-1/1b, Tirekhtyakh Formation. **J**, *Amorphognathus* sp., fragment of S? element, GIT 652-10, sample 112-5/4, Tirekhtyakh Formation. **K**, *Pseudooneotodus mitratus*, upper view, GIT 652-11, sample 112-1/1, Tirekhtyakh Formation. **L, M, Q, R**, *Kockelella* cf. *manitoulinensis*: L, inner lateral view of Pb element, GIT 652-12; M, outer lateral view of Pa element, GIT 652-13; Q, inner lateral view of M element, GIT 652-14; R, inner lateral view of Sc element, GIT 652-15; all elements from sample 109-2/2, Maut Formation. **N**, *Nordiodus?* sp., outer (N1) and inner (N2) lateral views, GIT 652-16, sample 115-6/3, Tirekhtyakh Formation. **O**, *Oulodus?* *panuarensis*, inner lateral view of M element, GIT 652-17, sample 110-1/3, Maut Formation. **P**, *Ozarkodina* ex gr. *oldhamensis*, lateral view of Pa element, GIT 652-18, sample 110-1/3, Maut Formation. **S, T**, *Distomodus* cf. *kentuckyensis*: S, inner lateral view of M element, GIT 652-19; T, posterior view of Sb element, GIT 652-20; both specimens from sample 109-4/3, Maut Formation. **U, V**, *Ozarkodina* sp.: U, lateral view of Pa element, GIT 652-21, sample 109-4/3; V, posterior view of Sa element, GIT 652-22; both specimens from sample 109-5/3b; both specimens from Maut Formation. **W, X, AA, BB**, *Walliserodus* cf. *curvatus*: W, lateral view of asymmetrical dyscritiform element, GIT 652-23; X, lateral view of symmetrical dyscritiform element, GIT 652-24; AA, inner lateral view of curvatiform element, GIT 652-25; BB, inner lateral view of multicostatiform element, GIT 652-26; W and X from sample 109-2/2, AA and BB from sample 109-4/3; all specimens from Maut Formation. **Y**, *Decoriconus* sp., lateral view, GIT 652-27, sample 109-4/3, Maut Formation. **Z, CC, DD**, *Oulodus?* sp.: Z, inner lateral view of Pa element, GIT 652-28; CC, inner lateral view of Sc element, GIT 652-29; DD, inner lateral view of Pb element, GIT 652-30; all specimens from sample 109-4/3, Maut Formation.



Two specimens illustrated by Zhang & Barnes (2007, fig. 10: 1 and 3) as elements of *Oulodus* sp. 1 are very similar to, respectively, Pb and M elements of *Ozarkodina excavata puskuensis* Männik; one specimen (Zhang & Barnes 2007, fig. 10: 2) seems to be an M element of *Aspelundia? expansa* Armstrong. It is most probable that both *O. e. puskuensis* and *A.? expansa* occur in the Mirny Creek section. In Estonia these taxa are known from (late) Rhuddanian and Aeronian strata (Männik 2003, 2010). A specimen of *A.? expansa* in sample SIB79-33 indicates that the lower boundary of the *A.? expansa* conodont Zone lies below this level.

Zhang & Barnes (2007, fig. 10: 31–35) recorded an unusual occurrence of a Telychian taxon in the Mirny Creek section: *Pterospathodus amorphognathoides amorphognathoides* Walliser in the strata corresponding to the lower *Coronograptus cyphus* Zone (sample SIB79-48; Member 79 of the Maut Formation). The two largest specimens (Zhang & Barnes 2007, fig. 10: 34 and 35) possess a wide distinct basal platform characteristic of *P. a. amorphognathoides*. This unusual find confirms that certain parts of the Mirny Creek section are tectonically complicated. As noted above, the same conclusion has been reached also by earlier studies (Oradovskaya & Sobolevskaya 1979).

The general composition of conodont faunas studied by us agrees with the view of Zhang & Barnes (2007) that the Late Ordovician assemblage in the Mirny Creek section is closest to that of the North Atlantic Realm. A few taxa (e.g. *Belodina*), which Zhang & Barnes (2007) referred to as characteristic of the Midcontinent Realm, are not abundant in the Mirny Creek section but are quite common in the Baltic faunas. The single possible fragment of *Aphelognathus* (one of the most frequent taxa in the Midcontinent Realm), identified from sample SIB79-40 (Zhang & Barnes 2007, fig. 7: 8), seems to be a fragment of *Amorphognathus*. The Silurian conodont assemblage is also similar to that of the Baltic region. The only exceptions are *Ozarkodina* cf. *O. n. sp. B* Simpson & Talent identified by Zhang & Barnes (2007) from the Mirny Creek section (Fig. 4) and *Ozarkodina* cf. *O. masurenensis* Bischoff recognized by the same authors from the Maut Formation (Unit T, Member 11) in the Ina River section (located close to Mirny Creek). Both taxa are characteristic of the Silurian faunas of Australia.

## DISCUSSION

### Dating of some key points of the Mirny Creek carbon isotope trend and stratigraphical implications

The Mirny Creek section, at least in our study interval, is in general firmly dated by graptolites (Koren' et al.

1983; Koren' & Sobolevskaya 2008) and only a few key points need to be discussed in more detail. Besides, our aim is to promote trustworthy correlation of sections of different facies origin where integrated chemo- and biostratigraphy has good prospects. In this context we consider here also some brachiopod and conodont data.

The upper Katian part of the Mirny  $\delta^{13}\text{C}$  curve is safely dated by graptolites of the *Appendispinograptus supernus* Biozone (Fig. 3). Conodonts are rare and occur too sporadically in this interval to allow precise dating of rocks but general composition of fauna indicates that it is of Katian age and partly not contradicting the *Amorphognathus ordovicicus* Zone interval as shown in Fig. 2. Several tabulate corals and brachiopods are found in this part of the section, at a few levels in limestone beds (members 58, 60, 62). Among brachiopods, *Holorhynchus* ex gr. *giganteus* occurring in members 60 and 62 is worth to mention. This taxon is also known from a similar pre-Hirnantian stratigraphic level (Pirgu Regional Stage) in Baltoscandia (Brenchley et al. 1997; Kaljo et al. 2008).

Identification of the Katian–Hirnantian boundary within the Tirekhtyakh Formation is more problematic. Graptolites (e.g. *Appendispinograptus supernus*, *Paraorthograptus pacificus* and *Normalograptus ojsuensis*) occurring in Unit P (Fig. 3; Koren' et al. 1983; Koren' & Sobolevskaya 2008) are known elsewhere also from the Hirnantian (Chen et al. 2006; Melchin & Holmden 2006; Mitchell et al. 2011). *Normalograptus extraordinarius* appears in the basal part of Member 68. Identification of this taxon at the base of Member 67 (sample 107-1/1) by Koren' et al. (1983) was later revised. However, as discussed above, the  $\delta^{13}\text{C}$  curve in Member 67 demonstrates a typical 'rising limb' of the HICE. This discrepancy needs explanation. Member 67 consists of pack- and grainstones, partly with poorly rounded clasts of biohermal limestone that are surely not very likely to contain graptolites. Here we wish to point out the first appearance datum (FAD) of *N. ojsuensis* ca 2 m below the base of Member 67. In the Hirnantian GSSP section at Wangjiawan North the FAD of *N. ojsuensis* is 4 cm below the FAD of *N. extraordinarius* (Chen et al. 2006). In terms of the Mirny locality, 4 cm mean ca 400 cm and we could expect the latter species be found in the middle of Member 67, but rocks are unfavourable. Kaljo et al. (2008) mentioned that the actual increase in the HICE values began in several sections in China slightly below the *N. extraordinarius* Biozone (i.e. in the *Diceratograptus mirus* Biozone; Chen et al. 2006; see also LaPorte et al. 2009 for Nevada). This seems to be a case also in the Mirny Creek section and consequently the Katian–Hirnantian boundary might be correlated with the middle of Member 67. Still, a more realistic position of the boundary is at the base of

Member 68, as shown in Fig. 3 according to Koren' & Sobolevskaya (2008).

Another important point that should be made clear is the age (level) of the main peak of the HICE. Beginning with the paper by Melchin et al. (2003) that revised graptolite biozonation in the Dob's Linn (Scotland) GSSP section for the base of the Silurian System, it has widely been accepted that the main peak of the HICE is correlated with the lower part of the *N. persculptus* Biozone. The peak value of  $\delta^{13}C_{org}$  was measured 108 cm above the base of the *N. persculptus* Biozone and 172 cm from the O/S boundary, i.e. a bit less than 40% from the bottom of the biozone (Underwood et al. 1997 revised). On the basis of graphic correlation Chen et al. (2006) located the bottom of the *N. persculptus* Biozone in the Wangjiawan Riverside section within the Kuanyinchiao Bed and the peak of the  $\delta^{13}C_{org}$  trend was thought to be in the lower part of the biozone. It is not a very exact, but still useful hint that has been used in several correlation schemes (Melchin & Holmden 2006; Kaljo et al. 2008; Achab et al. 2011). Gorjan et al. (2012) published the first  $\delta^{13}C_{carb}$  curve (reproduced here in Fig. 6) from the same South China section, which differs greatly from the general understanding of the HICE, including its shape and correlation. The rising half of

the excursion is quite typical with the highest values (just below +2‰) occurring high in the *N. extraordinarius* Biozone, but the continuation in the *N. persculptus* Biozone is unusual, showing a much lower peak that reaches only a bit over -1‰. This curve might be important for further discussion of correlation aspects and casts an example to the earlier warnings (Munnecke et al. 2010) about problems with stratigraphic use of organic carbon trends. Besides, despite a rather detailed discussion of possible causes disturbing the normal  $\delta^{13}C$  values of the isotope signal, the current low values in the upper HICE remain obscure or we can accept that it might be a result of co-effect of different reasons.

The Mirny Creek section allows some precise indications – the maximum  $\delta^{13}C$  values occur practically midway from the *N. persculptus* Biozone bottom (52%). All sections noted above were graptolite-bearing ones. Baltic carbonate rocks with shelly faunas demonstrate more variation in the peak position: the peak of the HICE is at the level of 25% from the bottom of the whole Hirnantian in the Ruhnu section, at 53% in the Kardla section and at 63% in the Stirnas section. The last value is closest to that of the Mirny Creek section if the peak distance is measured from the bottom of the *N. extraordinarius* Biozone where we got 71%.

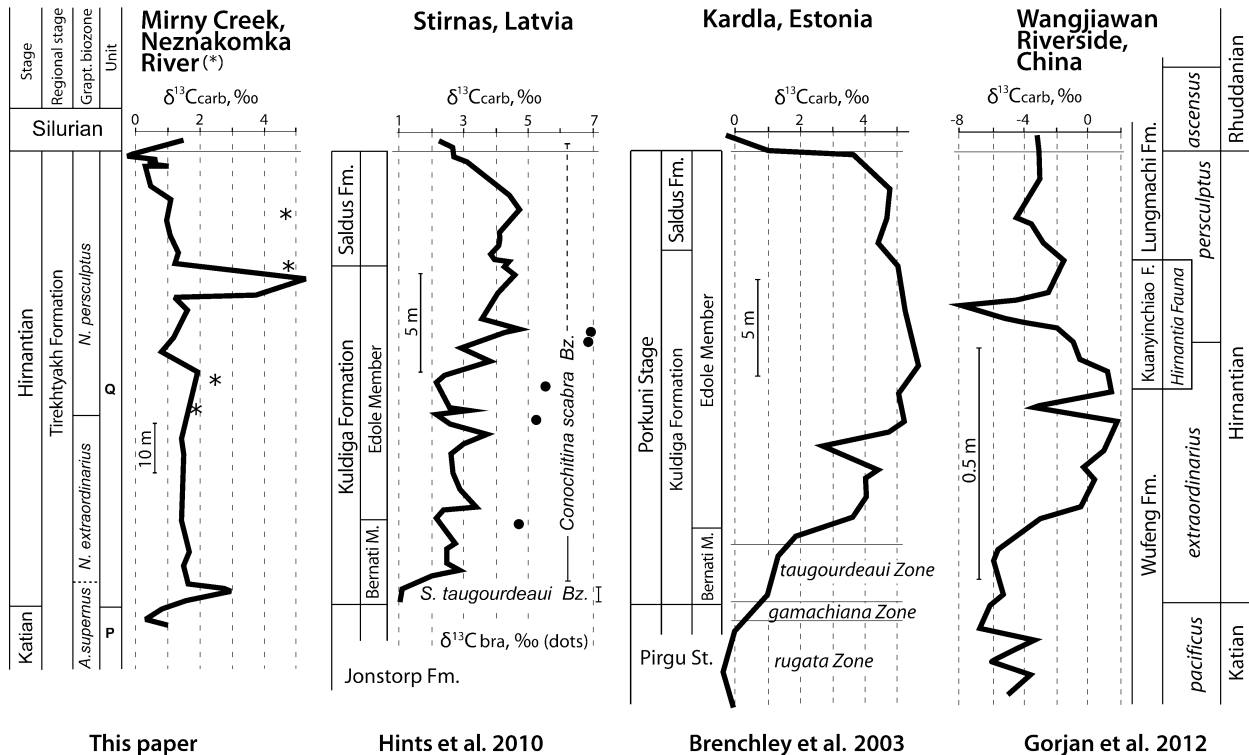


**Fig. 6.** Comparison of the Mirny Creek area, Baltic and Chinese generalized Hirnantian carbon isotope trends. Note that all curves are modified from originals, the vertical scale of the drawing is unified, differences in thicknesses of rocks can be followed using the scale bar. The Mirny Creek curve was first published by Kaljo & Martma (2011).

The upper boundary of the HICE in the Mirny Creek section is well defined by the FAD of *Akidograptus ascensus* in the lowermost part of the Maut Formation (in Member 74, Fig. 3). Conodonts characteristic of the Silurian (*Kockelella* cf. *manitoulinensis*, *Dapsilodus* sp. n. R, *Walliserodus* cf. *curvatus*) appear in the upper part of this member (sample 109-2/2-5; Fig. 4).

### Shape of the $\delta^{13}\text{C}$ curve: some comparisons

The Mirny Creek carbon isotope trend described above (Figs 3, 6) consists of a short and rather typical pre-Hirnantian (late Katian) part and a much longer one, which is surely the widely known HICE. Besides, a highly specific excursion is represented there, which at first glance seems to be rather different from the other end-Ordovician  $\delta^{13}\text{C}_{\text{carb}}$  curves described in the Baltic (Kaljo et al. 2001, 2008; Brenchley et al. 2003) or elsewhere (Finney et al. 1999; Kump et al. 1999; Bergström et al. 2006, 2012; LaPorte et al. 2009).

With regard to similarities of curves, we should surely mention the pre-Hirnantian (upper Katian) part of the Mirny Creek trend consisting of a plateau of low-level values varying close to 1‰ in Unit O (see above, Fig. 3). This plateau largely resembles the curves from synchronous rocks of western Anticosti (Long 1993; Jones et al. 2011) and the Baltic area (Ainsaar et al. 2010) or even a  $\text{C}_{\text{org}}$  curve by Zhang et al. (2009) from the Honghuayuan section in China. The interval of increasing values (Unit P) with a peak in the bottom of Unit Q (Figs 3, 6) is also highly similar. Such a ‘rising limb of the HICE’ is well known in several areas (Ainsaar et al. 2010; Hints et al. 2010). Higher in the Mirny Creek section follows a rather smooth plateau of values up to the main peak in Member 70. This plateau is different from the lower part of the HICE in several sections, e.g. Kardla, Estonia (Kaljo et al. 2001) and Nevada (e.g. Finney et al. 1999). However, it has much in common with the corresponding interval in the Stirnas-18 section of Latvia (Hints et al. 2010), only values in the latter are more variable (similarities are better seen by means of medians or trendline). The same could be told about the upper part of the HICE at Mirny Creek where we recognized some similarities with the Taagepera, Estonia (Brenchley et al. 2003) and Stirnas, Latvia (Hints et al. 2010) curves.

Besides those similarities we should note also a common difference –  $\delta^{13}\text{C}$  values in both plateaus (before and after the main peak) are as a rule at least 1‰ lower than, e.g., in the Stirnas section, and the curve is nearly horizontal, not trending as in many other places. Another difference, actually tied to the horizontal plateaus, is the shape of the main peak – it is narrow,

rising from a plateau, and not like many pyramidal excursions. The peak values seem to be more or less normal (considering the relative height of the peak), but surely addition of 1‰ would also be normal. It seems that there is a general but case-specific reason that caused the shape of the excursion. One possible reason might be insufficient density of sampling (see below). As mentioned above in the ‘Results’ chapter, data from the Neznakomka River showing a much wider peak refer to a possible very local environmental reason or gaps in the section similar to those noted by Bergström et al. (2006) elsewhere.

### Shape of the $\delta^{13}\text{C}$ curve: possible reasons

Here we focus our attention on the main features of the  $\delta^{13}\text{C}$  curve in the Mirny Creek section, leaving aside the above similarities. Actually, there are two peaks in the HICE: a medium-sized peak at the very beginning and a much higher major one, separated from the former by a slightly elevated plateau. The HICE ends with another plateau. Such plateaus, especially the rather long one between the peaks, were observed for the first time. A small set-back of  $\delta^{13}\text{C}$  values, revealed by a couple of analyses after the initial increase in the HICE, can be seen in both kinds of curves ( $\text{C}_{\text{carb}}$  and  $\text{C}_{\text{org}}$ ) presented by several authors (Finney et al. 1999; Kaljo et al. 2001; Bergström et al. 2006; Chen et al. 2006; Gorjan et al. 2012). Based on this set-back, Fan et al. (2009) even distinguished peaks 1 and 2. Data from the Neznakomka River (although insufficiently precisely positioned) soften to some extent the Mirny Creek  $\delta^{13}\text{C}$  excursion pattern, but the presence of the wide plateau still needs explanation.

The first striking circumstance that may affect the curve is the thickness of Hirnantian rocks and the very high accumulation rate of sediments. This might have had some influence if the isotope trend had a punctuated character instead of continuous one. The thickness of the Hirnantian is ca 90 m at Mirny Creek and reaches ca 70 m in Copenhagen Canyon, Nevada (rather close to the figure at Mirny Creek), but no plateau pattern is observed in the latter region (Finney et al. 1999). Neither has such a plateau been recorded in much thinner sections in the Baltic area and elsewhere (Kaljo et al. 2001, 2008; Brenchley et al. 2003; Bergström et al. 2006). It seems that a high sedimentation rate cannot be the only reason for the origination of the plateau pattern and another local reason should be looked for. The Neznakomka River data refer to facies differences – much higher values are tied to purer carbonate rocks (limestones) with a lesser content of the argillaceous and silt component. The same relationship is obvious

from Fig. 6, where the Wangjiawan curve documents much smaller  $\delta^{13}\text{C}$  changes (2–3‰) in deep-water rocks with a low calcite content (Gorjan et al. 2012) than in the Kardla carbonate-rich mid- to shallow shelf section (relative amplitude of values 4–5‰). Such a pattern has been observed in several occasions in the Baltic shoreward transects and elsewhere (Kaljo et al. 1998; Munnecke et al. 2003).

The isotope excursions of the Mirny Creek and Stirnas sections (Fig. 6) show a certain similarity, when leaving aside a stronger variability of the first third of the latter curve. The beginning of both excursions is identical. A long plateau follows in the Mirny Creek and a variable interval in the Stirnas section, where the mean value reaches the 2.7‰ level, i.e. ca 1.2‰ higher than the mean of the plateau at Mirny Creek. Both the plateau and the variable interval end with a pronounced low, where the values begin to rise stepwise up to the highest peak of the trend. These main peaks are rather similar – both close to 5‰, but reaching 7‰ in the Stirnas section on the basis of  $\delta^{13}\text{C}_{\text{bra}}$ . Both peaks occur in the upper half of the Hirnantian, but a little higher in the Mirny Creek section (74% from the bottom) in the middle of the *N. persculptus* Biozone. At Mirny Creek the peak is followed by a steep drop of values (ca 4‰) and then by a smoother decline of the curve. In the Stirnas section the peak is followed by another variable plateau with a mean value of 4.1‰ within the next 8 m and only then by a clearly declining limb. The two uppermost analyses from the Neznakomka River shown in Fig. 3 suggest an analogous wider excursion peak also in that area. At the same time these samples raise a question why the main peak is so narrow (only 3–4 m) and steep at Mirny Creek. Having in mind several truncated sections demonstrated by Brenchley et al. (2003) from the Baltic and Anticosti (also Achab et al. 2011), we suggest that a part of the Mirny Creek section just above the peak may be missing.

Another shape of the  $\delta^{13}\text{C}_{\text{carb}}$  curve is represented here by the Kardla section (Fig. 6), and is widely known in the Monitor Range, Nevada and elsewhere (Finney et al. 1999; Saltzman & Young 2005; Bergström et al. 2006; Kaljo et al. 2007; LaPorte et al. 2009). This type of excursion is biostratigraphically most convincingly constrained by graptolites in the Central Nevada sections. Organic carbon data are often more variable (Melchin & Holmden 2006; Fan et al. 2009; Zhang et al. 2009; Munnecke et al. 2010). We do not go into details, because according to the conodont colour alteration index (CAI 4–5), the Mirny Creek sections are heated up to 300–400 °C (Zhang & Barnes 2007; this paper) and therefore not suitable for  $\text{C}_{\text{org}}$  analysis. On the other hand, graptolite-bearing rocks, usually analysed for  $\text{C}_{\text{org}}$ ,

do not cause normally serious dating problems and can help through cautious chemostratigraphic correlation.

Summarizing the above discussion, we can note that the well-dated main peak of the HICE is usually located in the lower to middle part of the *N. persculptus* Biozone. The whole excursion may have 2–3 lower-level secondary peaks or be subdivided into parts by one or two negative shifts (Fig. 6). The  $\delta^{13}\text{C}_{\text{carb}}$  and  $\delta^{13}\text{C}_{\text{org}}$  curves are partly trending in harmony, but mostly they are not and the latter curve is as a rule more variable. The  $\delta^{13}\text{C}_{\text{carb}}$  curve recently published from the Wangjiawan Riverside section (Gorjan et al. 2012) shows the main peak in the middle or upper part of the *N. extraordinarius* Biozone (Fig. 6) and much lower values in the *N. persculptus* Biozone, but reasons for the latter are unclear. Therefore we think that a general shape of the HICE trend is pyramidal, which is peaking in the *N. persculptus* Biozone. Differences in the values and shape of the actual curve at different localities depend on local environmental conditions, sometimes modifying the global signal rather strongly.

As the HICE is a synchronous global event of relatively short duration (1–2 Ma), we can believe that peak values of the  $\delta^{13}\text{C}$  excursion were also reached more or less synchronously within a brief time interval. We should also note complications with recognizing the peak level of an excursion – at some locations this may not be self-evident at all. If this is the case, then, most generally speaking, a normal carbon isotope excursion is a smooth positive curve with one or several peaks. Abrupt changes in values (steep limbs of peaks and shifts) point to a disruption of the process, a hiatus or something else.

## CONCLUSIONS

1. The longest Hirnantian  $\delta^{13}\text{C}$  trend in the Mirny Creek section has a highly specific shape but is well constrained by graptolite biostratigraphy. The beginning of the trend is dated by the FAD of *N. extraordinarius*, but it might commence slightly below this level. The main peak occurs nearly in the middle of the *N. persculptus* Biozone. A few additional samples from the Neznakomka River suggest a somewhat wider peak interval than at Mirny Creek.
2. Detailed comparison of the Mirny Creek and Stirnas (Latvia)  $\delta^{13}\text{C}$  curves shows their general similarity despite great specifics of both trends. This correlation facilitates the linking of the Baltic chitinozoan and conodont biostratigraphy with the global graptolite biozonal standard.

3. Correlation of the  $\delta^{13}\text{C}$  trends known from China, Baltica and North America with that at Mirny Creek shows a great variety of shapes of the curve, but generally speaking a pyramidal excursion is most common. The rising limb of the curve, if represented, commenced everywhere at the very beginning (or slightly earlier) of the *N. extraordinarius* Biozone, in terms of Baltica, at the bottom of the Porkuni Regional Stage. Peak values of the HICE may be reached in a broad interval in the middle of the Hirnantian. Their actual values depend on environmental conditions at the site.

**Acknowledgements.** This paper was initiated together with T. N. Koren', but compiled much later. Authors are indebted to M. M. Oradovskaya and A. A. Suyarkova for assistance with information about samples and G. Baranov for technical help with graphics. We thank the referees S. M. Bergström and A. Munnecke for detailed constructive reviews. The study was partly supported by the Estonian Research Council (grants Nos 8182, 8907, 9039, project SF0140020s08). This paper is a contribution to IGCP project 591.

## REFERENCES

- Achab, A., Asselin, E., Desrochers, A., Riva, J. & Farley, C. 2011. Chitinozoan biostratigraphy of a new Upper Ordovician stratigraphic framework for Anticosti Island, Canada. *Geological Society of America, Bulletin*, **123**, 186–205.
- Ainsaar, L., Kaljo, D., Martma, T., Meidla, T., Männik, P., Nõlvak, J. & Tinn, O. 2010. Middle and Upper Ordovician carbon isotope chemostratigraphy in Baltoscandia: a correlation standard and clues to environmental history. *Palaeogeography, Palaeoclimatology, Palaeoecology*, **294**, 189–201.
- Bergström, S. M., Saltzman, M. M. & Schmitz, B. 2006. First record of the Hirnantian (Upper Ordovician)  $\delta^{13}\text{C}$  excursion in the North American Midcontinent and its regional implications. *Geological Magazine*, **143**, 657–678.
- Bergström, S. M., Lehnert, O., Calner, M. & Joachimski, M. M. 2012. A new upper Middle Ordovician–Lower Silurian drillcore standard succession from Borenskult in Östergötland, southern Sweden: 2. Significance of  $\delta^{13}\text{C}$  chemostratigraphy. *GFF*, **134**, 39–63.
- Brenchley, P. J., Marshall, J. D., Hints, L. & Nõlvak, J. 1997. New isotopic data solving an old biostratigraphic problem: the age of the upper Ordovician brachiopod *Holorhynchus giganteus*. *Journal of the Geological Society, London*, **154**, 335–342.
- Brenchley, P. J., Carden, G. A., Hints, L., Kaljo, D., Marshall, J. D., Martma, T., Meidla, T. & Nõlvak, J. 2003. High resolution isotope stratigraphy of Late Ordovician sequences: constraints on the timing of bio-events and environmental changes associated with mass extinction and glaciation. *Geological Society of America, Bulletin*, **115**, 89–104.
- Chen, X., Rong, J. Y., Fan, J. X., Zhan, R. B., Mitchell, C. E., Harper, D. A. T., Melchin, M. J., Peng, P., Finney, S. C. & Wang, X. F. 2006. The global boundary stratotype section and point (GSSP) for the base of the Hirnantian Stage (the uppermost of the Ordovician System). *Episodes*, **29**, 183–196.
- Cocks, L. R. M. & Torsvik, T. 2004. Major terranes in the Ordovician. In *The Great Ordovician Biodiversification Event* (Webby, B. D., Paris, F., Droser, M. L. & Percival, I. G., eds), pp. 61–67. Columbia University Press, New York.
- Fan, J., Peng, P. & Melchin, M. J. 2009. Carbon isotopes and event stratigraphy near the Ordovician–Silurian boundary, Yichang, South China. *Palaeogeography, Palaeoclimatology, Palaeoecology*, **276**, 160–169.
- Finney, S. C., Berry, W. B. N., Cooper, J. D., Ripperdan, R. L., Sweet, W. C., Jacobson, S. R., Soufiane, A., Achab, A. & Noble, P. 1999. Late Ordovician mass extinction: a new perspective from stratigraphic sections in central Nevada. *Geology*, **27**, 215–218.
- Gorjan, P., Kaiho, K., Fike, D. A. & Chen, X. 2012. Carbon and sulfur-isotope geochemistry of the Hirnantian (Late Ordovician) Wangjiawan (Riverside) section, South China: global correlation and environmental event interpretation. *Palaeogeography, Palaeoclimatology, Palaeoecology*, **337–338**, 14–22.
- Hints, L., Hints, O., Kaljo, D., Kiipli, T., Männik, P., Nõlvak, J. & Pärnaste, H. 2010. Hirnantian (latest Ordovician) bio- and chemostratigraphy of the Stirnas-18 core, western Latvia. *Estonian Journal of Earth Sciences*, **59**, 1–24.
- Jones, D. S., Fike, D. A., Finnegan, S., Fischer, W. W., Schrag, D. P. & McCay, D. 2011. Terminal Ordovician carbon isotope stratigraphy and glacioeustatic sea-level change across Anticosti Island (Quebec, Canada). *Geological Society of America, Bulletin*, **123**, 1645–1664.
- Kaljo, D. & Martma, T. 2011. Carbon isotope trend in the Mirny Creek Area, NE Russia, its specific features and possible implications of the Uppermost Ordovician stratigraphy. In *Ordovician of the World* (Gutierrez-Marco, J. C., Rabano, I. & Garcia-Bellido, D., eds), *Cuadernos del Museo Geominero*, **14**, 267–273.
- Kaljo, D., Kiipli, T. & Martma, T. 1997. Carbon isotope event markers through the Wenlock–Pridoli sequence in Ohesaare (Estonia) and Priekule (Latvia). *Palaeogeography, Palaeoclimatology, Palaeoecology*, **132**, 211–224.
- Kaljo, D., Kiipli, T. & Martma, T. 1998. Correlation of carbon isotope events and environmental cyclicity in the East Baltic Silurian. In *Silurian Cycles – Linkages of Dynamic Stratigraphy with Atmospheric, Oceanic and Tectonic Changes* (Landing, E. & Johnson, M. E., eds), *New York State Museum, Bulletin*, **491**, 297–312.
- Kaljo, D., Hints, L., Martma, T., Nõlvak, J. & Oraspõld, A. 2001. Carbon isotope stratigraphy in the latest Ordovician of Estonia. *Chemical Geology*, **175**, 49–59.
- Kaljo, D., Martma, T. & Saadre, T. 2007. Post-Hunnebergian Ordovician carbon isotope trend in Baltoscandia, its environmental implications and some similarities with

- that of Nevada. *Palaeogeography, Palaeoclimatology, Palaeoecology*, **245**, 138–155.
- Kaljo, D., Hints, L., Männik, P. & Nölvak, J. 2008. The succession of Hirnantian events based on data from Baltica: brachiopods, chitinozoans, conodonts, and carbon isotopes. *Estonian Journal of Earth Sciences*, **57**, 197–218.
- Koren', T. N. & Sobolevskaya, R. F. 2008. The regional stratotype section and point for the base of the Hirnantian Stage (the uppermost Ordovician) at Mirny Creek, Omulev Mountains, Northeast Russia. *Estonian Journal of Earth Sciences*, **57**, 1–10.
- Koren', T. N., Oradovskaya, M. M., Pylma, L. J., Sobolevskaya, R. F. & Chugaeva, M. N. 1983. *Granitsa ordovika i silura na severo-vostoke SSSR [The Ordovician and Silurian Boundary in the Northeast of the USSR]* (Sokolov, B. S., Koren', T. N. & Nikitin, I. F., eds). Nauka, Leningrad, 205 pp. [in Russian].
- Kump, L. R., Arthur, M. A., Patzkowsky, M. E., Gibbs, M. T., Pinkus, D. S. & Sheehan, P. M. 1999. A weathering hypothesis for glaciation at high atmospheric pCO<sub>2</sub> during the Late Ordovician. *Palaeogeography, Palaeoclimatology, Palaeoecology*, **152**, 173–187.
- LaPorte, D. F., Holmden, C., Patterson, W. P., Loxton, J. D., Melchin, M. J., Mitchell, C. E., Finney, S. C. & Sheets, H. D. 2009. Local and global perspectives on carbon and nitrogen cycling during the Hirnantian glaciation. *Palaeogeography, Palaeoclimatology, Palaeoecology*, **276**, 182–195.
- Long, D. G. F. 1993. Oxygen and carbon isotopes and event stratigraphy near the Ordovician–Silurian boundary, Anticosti Island, Quebec. *Palaeogeography, Palaeoclimatology, Palaeoecology*, **104**, 49–59.
- Loydell, D. K., Nestor, V. & Männik, P. 2010. Integrated biostratigraphy of the lower Silurian of the Kolka-54 core, Latvia. *Geological Magazine*, **147**, 253–280.
- Männik, P. 2003. Distribution of Ordovician and Silurian conodonts. In *Ruhnu (500) Drill Core* (Pöldvere, A., ed.), *Estonian Geological Sections*, **5**, 17–23.
- Männik, P. 2010. Distribution of Upper Ordovician, Llandovery and Wenlock conodonts. In *Viki Drill Core* (Pöldvere, A., ed.), *Estonian Geological Sections*, **10**, 21–24.
- Martma, T., Brazauskas, A., Kaljo, D., Kaminskas, D. & Musteikis, P. 2005. The Wenlock–Ludlow carbon isotope trend in the Vidukle core, Lithuania, and its relations with oceanic events. *Geological Quarterly*, **49**, 223–234.
- Melchin, M. J. & Holmden, C. 2006. Carbon isotope chemostratigraphy in Arctic Canada; sea-level forcing of carbon platform weathering and implications for Hirnantian global correlation. *Palaeogeography, Palaeoclimatology, Palaeoecology*, **234**, 186–200.
- Melchin, M. J., Holmden, C. & Williams, S. H. 2003. Correlation of graptolite biozones, chitinozoan biozones, and carbon isotope curves through the Hirnantian. In *Ordovician from Andes* (Albanesi, G. L., Beresi, M. S. & Peralta, S. H., eds), *INSUGEO, Serie Correlación Geológica*, **17**, 101–104.
- Mitchell, C. E., Štorch, P., Holmden, C., Melchin, M. J. & Gutiérrez-Marco, J. C. 2011. New stable isotope data and fossils from the Hirnantian Stage in Bohemia and Spain: implications for correlation and paleoclimate. In *Ordovician of the World* (Gutiérrez-Marco, J. C., Rábano, I. & Garcia-Bellido, D., eds), *Cuadernos del Museo Geominero*, **14**, 371–378.
- Munnecke, A., Samtleben, C. & Bickert, T. 2003. The Ireviken Event in the lower Silurian of Gotland, Sweden – relation to similar Palaeozoic and Proterozoic events. *Palaeogeography, Palaeoclimatology, Palaeoecology*, **195**, 99–124.
- Munnecke, A., Calner, M., Harper, D. A. T. & Servais, T. 2010. Ordovician and Silurian sea-water chemistry, sea level, and climate: a synopsis. *Palaeogeography, Palaeoclimatology, Palaeoecology*, **296**, 389–413.
- Nowlan, G. S. & Barnes, C. R. 1987. Application of conodont colour alteration indices to regional and economic geology. In *Conodonts: Investigative Techniques and Applications* (Austin, R. L., ed.), pp. 188–202. Ellis Howood Ltd., Chichester.
- Oradovskaya, M. M. & Sobolevskaya, R. F. 1979. *Guidebook to Field Excursion to the Omulev Mountains*. XIV Pacific Science Congress, Khabarovsk. Magadan Publishing House, 103 pp.
- Rong, J.-Y. & Harper, D. A. T. 1988. A global synthesis of the latest Ordovician Hirnantian faunas. *Transactions of the Royal Society of Edinburgh: Earth Sciences*, **79**, 383–402.
- Saltzman, M. R. & Young, S. A. 2005. Long-lived glaciation in the Late Ordovician? Isotopic and sequence-stratigraphic evidence from western Laurentia. *Geology*, **33**, 109–112.
- Schmitz, B. & Bergström, S. 2007. Chemostratigraphy in the Swedish Upper Ordovician: regional significance of the Hirnantian  $\delta^{13}\text{C}$  excursion (HICE) in the Boda Limestone of the Siljan region. *GFF*, **129**, 133–140.
- Underwood, C. J., Crowley, S. F., Marshall, J. D. & Brenchley, P. J. 1997. High-resolution carbon isotope stratigraphy of the basal Silurian Stratotype (Dob's Linn, Scotland) and its global correlation. *Journal of the Geological Society*, **154**, 709–718.
- Webby, B. D., Cooper, R. A., Bergström, S. M. & Paris, F. 2004. Stratigraphic framework and time slices. In *The Great Ordovician Biodiversification Event* (Webby, B. D., Paris, F., Droser, M. L. & Percival, I. G., eds), pp. 41–47. Columbia University Press, New York.
- Zhamoida, A. I. (Editor-in-chief). 1992. *Stratigraphic Code. Second edition*. Interdepartmental stratigraphic committee. St. Petersburg, 120 pp.
- Zhang, S. & Barnes, C. R. 2007. Late Ordovician to Early Silurian conodont faunas from the Kolyma terrane, Omulev Mountains, Northeast Russia, and their paleobiogeographic affinity. *Journal of Paleontology*, **81**, 490–512.
- Zhang, T. G., Shen, Y. N., Zhan, R. B., Shen, S. Z. & Chen, X. 2009. Large perturbations of the carbon and sulfur cycle associated with the Late Ordovician mass extinction in South China. *Geology*, **37**, 299–302.

## Lisandusi süsiniku isotoopide ja konodontide tundmisele Ordoviitsiumi ning Siluri piirikihtides Mirnõi oja paljandites Omulevi mägedes Kirde-Venemaal

Dimitri Kaljo, Peep Männik, Tõnu Martma ja Jaak Nõlvak

Ordoviitsiumi ajastu lõpul ja Siluri algul toimusid põhjalikud muutused tollases keskkonnas ning elustiku mitmekesisuses. Töös on käsitletud Mirnõi oja ja Neznakomka jõe kaldail paljanduvaid Ülem-Kati kuni Alam-Rhuddani karbonaatkivimeid (osalt biohermidega), mis vahelduvad graptoliite sisaldavate argilliitide ning aleuroliitidega. Mikrofossiile esineb harva, eriti Hirnanti lademe piires, kuid konodontid on sellest all- ja ülalpool mõnevõrra informatiivsed. Süsinikisotoopide suhte kõver Mirnõi oja Hirnanti läbilõikes (HICE) on seniuurituist pikim (90 m) maailmas ja väga spetsiifilise kujuga. HICE  $\delta^{13}\text{C}$  väärtuste kasv algab *Normalograptus extraordinarius*'e biotsooni alguses, järgneb peaaegu tõusuta pikk platoo ja väga kitsas kõrgpunkt (5,2‰) saavutatakse *N. persculptus*'e biotsooni alumises pooles. Pärast väärtuste järsku langust jätkub jälle pikk väikese kaldega platoo Siluri alguseni. Neznakomka jõe paljandite materjal näitab mõneti laiemat kõvera tippu. Võrdlus Baltikumi vastavate kõveratega näitab suurimat sarnasust Störnase (Läti) läbilõikega. Muude alade ja Mirnõi  $\delta^{13}\text{C}$  trendi võrdlus näitab, et tüüpiline HICE on püramiidja kujuga, mille tipp on enamasti *N. persculptus*'e biotsooni algosas. Kuna kohalik looduskeskkond võib globaalse signaali avaldumist oluliselt mõjutada, siis on tegelik kõvera kuju enamasti kirjeldatust mingil määral erinev.